O/Ni(111): Lateral interactions and binding-energy difference between fcc and hcp sites

C. Schwennicke and H. Pfnür
Institut für Festkörperphysik, Universität Hannover, Appelstraße 2, D-30167 Hannover, Germany
(Received 25 February 1997)

Based on low-energy electron diffraction structural investigations of ordered and disordered phases of O/Ni(111) that show that occupation of both fcc and hcp sites can be forced either by thermal activation or by coverage, the lateral interactions and the binding-energy difference of fcc and hcp sites are redetermined for this system by simulating the phase diagram with Monte Carlo simulations, concentrating on the coverage range between 0.25 and 0.33 ML. From a comparison of the temperature dependence of the occupation probability of fcc and hcp sites in experiment and simulations, the difference in binding energy between fcc and hcp sites is determined to be 46 meV. Using a minimum set of five pairwise lateral interactions, the experimental phase diagram in the investigated coverage range is reproduced in detail. Even the complex diffraction patterns experimentally observed in the domain-wall phase are well reproduced in the simulations. We show in particular that this phase is only stabilized by entropy. Critical properties of the $p(2\times2)$ order-disorder transition are discussed briefly. [S0163-1829(97)03540-6]

I. INTRODUCTION

The lateral interactions between adsorbed atoms on the surface as well as the binding-energy difference between different adsorption sites determine the existence and thermal stability of two-dimensional adsorbed phases and are therefore of great importance. Direct measurements of lateral interactions, however, have been possible for only a few examples using microscopic techniques such as field ion microscopy[1] or scanning tunneling microscopy.[2] In these experiments the distribution of distances between the interacting species such as adatoms on metal surfaces[1] or charged vacancies in compound semiconductors[2] is analyzed. These techniques, however, are limited to systems where the typical frequency of site changes is small compared to the data acquisition time. Single light adsorbate atoms on metal surfaces are often highly mobile in thermal equilibrium, making these techniques not suitable to determine lateral interactions.

The information about the microscopic lateral interactions is also contained in macroscopic thermodynamical properties, e.g., in the phase diagram. The phase diagram of two-dimensional chemisorbed systems (i.e., systems with negligible vapor pressure) contains information about the sequence of ordered phases as a function of concentration and about their thermal stability. Since for most practically relevant systems the equation of state cannot be solved analytically, the information about the (effective) lateral interactions is only available by model calculations. These calculations need as input the symmetry and the number of accessible sites per unit cell, properties that have to be determined experimentally.

For a number of adsorbate systems, in which site-specific adsorption occurs (lattice gas) and the lateral interactions are dominated by short-range interactions, the simulation of the phase diagram has been shown to allow an estimate of lateral interactions.[3] Even a relatively complex phase diagram can be simulated by just a single free parameter, i.e., a pair interaction, in the case of only one type of adsorption site, as demonstrated recently for the system S/Ru(0001) at low coverages.[4] For more complex systems where different adsorption sites are occupied, additional geometrical information as a function of temperature turns out to be essential since the phase diagram alone usually does not contain enough information to determine interaction parameters reliably.

O/Ni(111) is not only an almost classical system, on which a number of basic exploratory studies have been carried out in the past, including studies of the phase diagram,[5] lateral interactions,[6] geometry of various phases,[7,8] and critical phenomena.[9–11] In particular the latter investigations are still controversial, but we will not focus on them in this paper. Some of these studies have been carried out on the basis of an incomplete knowledge of the structure. Therefore, it seemed to be useful to reanalyze this system. Most structural studies of this system have been carried out in the recent past, including the analysis of thermally disordered layers. At a coverage of 0.25 monolayer (ML) our low-energy electron diffraction (LEED) analysis showed that the occupation of the hcp site can be thermally activated close to and above the order-disorder phase transition.[12] At higher coverages it is possible to occupy hcp sites even in a static disordered phase at low temperatures,[13] whereas in the long-range-ordered $p(2\times2)$ and $(\sqrt{3}\times\sqrt{3})R30°$ structures only fcc sites are occupied.[7,8]

In this paper we extend the analysis of the phase diagram by Monte Carlo simulations to the recent structural data available from experiment. We will show that the additional structural information from our LEED studies of the disordered phases of O/Ni(111) helps to overcome some ambiguities in the determination of interaction parameters for such a comparatively complex adsorption system. For example, we will show that the binding-energy difference between fcc and hcp sites can be accurately determined by comparing the temperature dependence of occupation probabilities of fcc and hcp sites in simulation and experiment.

The outline of the paper is the following. We will first describe the lattice-gas model we used in the simulations.

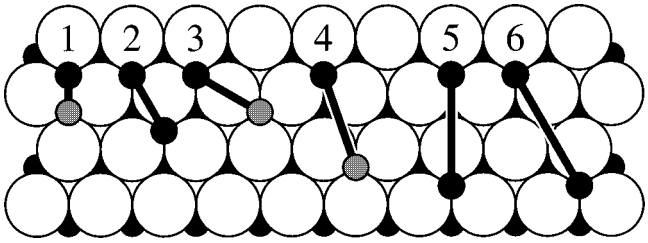

FIG. 1. Pair interactions included in the Hamiltonian of Eq. (1). Black-filled circles are adsorbate atoms in fcc sites, gray-filled circles atoms in hcp sites. Pair interactions between two atoms in hcp sites were assumed to be identical to the corresponding interactions between atoms in fcc sites.

Next, the determination of interaction energies by a fit to the experimental data is presented, which is the main subject of this paper. The experimental inputs used are the phase diagram itself as well as the data from the detailed LEED structural analyses. Finally, we will briefly describe the investigation of the critical properties of the order-disorder phase transition of the $p(2\times2)$ structure.

II. MODEL

In order to simulate the thermodynamic properties of O/Ni(111) at coverages above 0.25 ML one has to take into account that fcc and hcp sites are occupied. Therefore, Monte Carlo simulations were performed on a honeycomb lattice containing two adsorption sites per unit mesh. The minimum number of necessary interactions that has to be used in a lattice-gas model is determined by the structures that occur in the experiment. Two long range-ordered structures, a $p(2\times2)$ and a $(\sqrt{3}\times\sqrt{3})R30°$ structure, have been found for O/Ni(111). Therefore, we included all pair interactions into the simulations corresponding to distances $\leqslant 2a$, where $a=2.49$ Å is the nearest-neighbor distance on the Ni(111) surface. Figure 1 shows all lateral interactions e_1 to e_6 included in our lattice-gas model. In order to find the simplest possible model that describes the experimentally determined phase diagram, we assumed that pairwise interactions depend only on the distance between the adsorbate atoms, but not on the binding sites. Further n-particle interactions ($n\geqslant 3$) not considered in our model turn out to be unnecessary. Since oxygen adsorbs exclusively on fcc sites in the well-ordered $p(2\times2)$ and $(\sqrt{3}\times\sqrt{3})R30°$ structures at low temperatures,[7,8] a finite binding-energy difference h between fcc and hcp sites was included in the simulations. The Hamiltonian of the lattice-gas model is therefore given by

$$H=e_1\sum_{\mathrm{NN}} c_ic_j+\cdots+e_6\sum_{\mathrm{NNNNNN}} c_ic_j+h\sum_{\mathrm{hcp}} c_i, \quad (1)$$

where $c_i=0,1$ is the occupation number of the lattice site i and the sums are taken over nearest-neighbor (NN) pairs, next-nearest-neighbor (NNN) pairs, etc. The same model Hamiltonian was used in Ref. 6.

The interaction e_1 corresponds to a very small distance between adsorbate atoms that would result in a large overlap of atomic wave functions. The necessary activation energy to occupy this distance makes its occurrence highly unlikely.

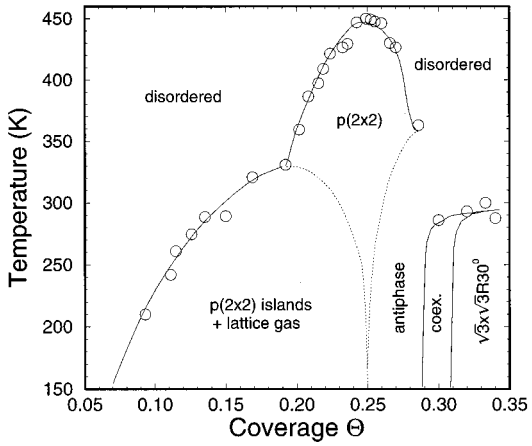

FIG. 2. Experimental phase diagram of the system O/Ni(111). The data points mark the measured transition temperatures for various coverages and phases. Phase boundaries are marked by solid lines as far as measured, whereas dotted lines indicate necessary continuations, which are not quantitative.

Therefore, this distance was excluded in the simulations. The interaction e_2 was set to 1 and defines the energy scale. Absolute energies can be determined in the final step by comparing experimental and simulated transition temperatures of the order-disorder phase transition of the $p(2\times2)$ structure. The remaining interactions as well as the binding-energy difference of fcc and hcp sites were fitted to experimental data.

All simulations were done at constant coverage, i.e., Kawasaki kinetics was used.[14] Each Monte Carlo step (MCS) includes a test of a site change at each lattice site. Lattice sites were selected using a checkerboard algorithm. The lattice used in the simulations had a rectangular shape containing $2N\times N$ lattice sites ($N\times N$ for each type of adsorption site) with periodic boundary conditions in the x and y directions. For the simulation of the phase diagram a lattice of 96×48 lattice sites was used. The surface was initialized randomly. About 10^5 MCS per data point were usually sufficient to study the phase diagram if critical properties of the phase transitions were not analyzed.

III. PHASE DIAGRAM

The phase diagram of O/Ni(111) was experimentally investigated by Kortan and Park[5] and could be well reproduced by Voges.[15] For easier comparison with the results of the simulation, we show our data in Fig. 2. At low temperatures a coexistence of lattice gas and of $p(2\times2)$ islands at coverages below 0.25 ML exists, which ends at the high-coverage side at the phase boundary to a homogeneous long-range ordered $p(2\times2)$ phase that is stable at coverages close to 0.25 ML. At coverages $\Theta>0.27$ ML a domain wall phase has been observed that is characterized by a broadening of (1/2,0) and a splitting of (1/2,1/2) diffraction spots. At even higher coverages of about 0.33 ML a well-ordered $(\sqrt{3}\times\sqrt{3})R30°$ structure was found in the experiment. Also, a small coexistence region of $(\sqrt{3}\times\sqrt{3})R30°$ and the domain wall structure was found, in agreement with Ref. 5. As mentioned, only fcc sites are occupied in the well-ordered $p(2\times2)$ and $(\sqrt{3}\times\sqrt{3})R30°$ structures at low

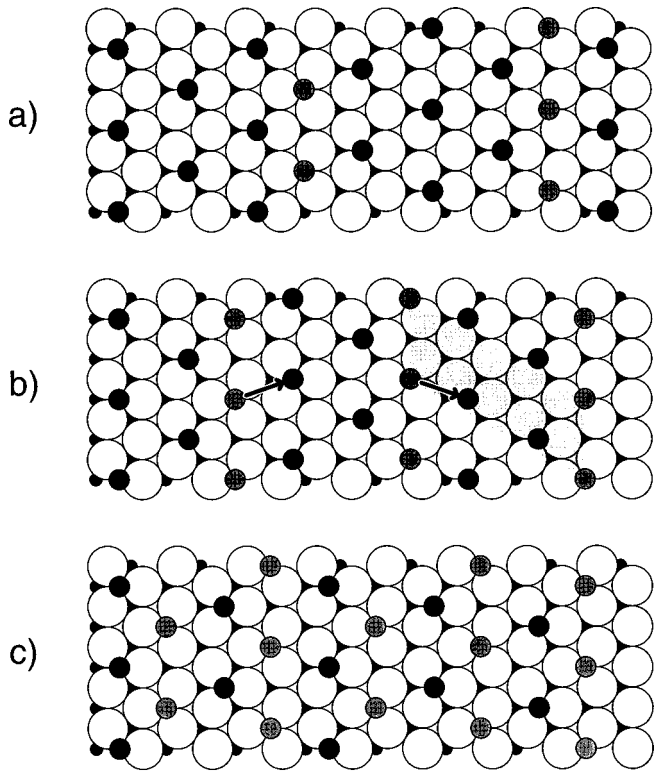

FIG. 3. One-dimensional model of the domain walls observed for O/Ni(111) at coverages $\Theta > 0.25$ ML. $p(2\times2)$ domains with oxygen atoms in fcc sites (black-filled circles) are separated by rows of single-atom width with hcp sites (gray-filled circles) occupied. The coverages are (a) $\Theta = 2/7$ ($w = 1/3$), (b) $\Theta = 3/10$ ($w = 1/2$), and (c) $\Theta = 1/3$ ($w = 1$). Note that the domain-wall structure was only observed up to a coverage of about 0.31 ML in the experiment at low temperatures.

temperatures.[7,8] However, the occupation of hcp sites can be activated at temperatures close to and above the order-disorder phase transition at the ideal coverage of the $p(2\times2)$ structure.[12]

At the intermediate coverage of 0.3 ML our own results show[12] that fcc and hcp sites are occupied even at rather low temperatures. This, however, is most likely not the ground state (see below). After an explicit determination of the site occupation probability of hcp and fcc sites in this phase and the analysis of relative phases between these sites,[13] the complex diffraction patterns observed in the experiment could be well reproduced if we assumed a random network of characteristic domain walls on the surface at this coverage. A simplified and idealized one-dimensional model of the domain-wall structure is shown in Fig. 3 for different coverages. As seen in Fig. 3, the $p(2\times2)$ domains with only fcc site occupation are separated by straight domain walls in which hcp sites are occupied. As the coverage is increased from 1/4 to 1/3, the density of domain walls and therefore the fraction of adsorbate atoms in hcp sites increase. Experimentally, a $(\sqrt{3}\times\sqrt{3})R30°$ structure is formed at coverages above ≈ 0.31 ML and temperatures below 300 K. The saturation density of domain walls at a coverage of 1/3 can only be observed in the experiment at temperatures above 300 K, i.e., in the disordered state. Parallel to the domain walls, the $p(2\times2)$ distance between adsorbate atoms is maintained for atoms in both fcc and hcp sites. The necessary compression at higher coverages is achieved by a smaller distance between adsorbate atoms perpendicular to the domain walls. Comparing our hard-ball model with Fig. 1, the interaction energies e_4 and e_6 and the binding-energy difference h determine the ground-state energy of such a domain-wall structure. The energetic ground-state energy per atom of the ordered $p(2\times2)$ and $(\sqrt{3}\times\sqrt{3})R30°$ phases is simply given by $3e_6$ and $3e_5$, respectively.

In order to determine the energetic parameters that are able to describe the full phase diagram of O/Ni(111), we successively determined the possible range of the different interaction energies. As just mentioned, e_1 was set to infinity and $e_2 = 1$ defines the energy scale. The distance corresponding to the interaction e_3 does not occur in the energetic ground state at any coverage. Thus e_3 has an influence only on the thermal stability of the different phases, but not on the sequence of phases occurring in the energetic ground state as a function of coverage. It turned out that the critical temperatures of the $p(2\times2)$ and the $(\sqrt{3}\times\sqrt{3})R30°$ phase can be adjusted by a variation of the other interaction energies as well, so we chose a value of $2/3e_2$ for the interaction energy e_3 and did not further vary this value. This value guarantees the monotonic decay of interaction energies as a function of the distance between adsorbate atoms. Nevertheless, we are still able to provide a lower bound for the value of e_3, which will be derived later in this section. The remaining parameters e_4, e_5, e_6, and h, however, have to fulfill several conditions in order to reproduce the experimentally observed sequence of phases at low temperatures, which will be derived in the following.

We will first consider the condition for the existence of the ordered $p(2\times2)$ and $(\sqrt{3}\times\sqrt{3})R30°$ phases. As shown by LEED structural analyses, only fcc sites are occupied in these structures at low temperatures. Even if only a single type of threefold hollow site is occupied competing phases can occur. For example, for the system O/Ru(0001), a $p(2\times2)$ and a $p(2\times1)$ but no $(\sqrt{3}\times\sqrt{3})R30°$ structure has been found.[16] It can be easily shown that the condition for the existence of a $(\sqrt{3}\times\sqrt{3})R30°$ structure in the energetic ground state is given by

$$e_5 < 0.2e_2 + \frac{6}{5}e_6; \tag{2}$$

otherwise a coexistence of a $p(2\times2)$ and a $p(2\times1)$ phase is energetically more favorable than a $(\sqrt{3}\times\sqrt{3})R30°$ structure at a coverage of 1/3 ML.[16] The value of e_5 is actually further restricted to a value close to $0.1e_2$ by the stability of these two phases, i.e., by the ratio of maximum transition temperatures between $p(2\times2)$ and $(\sqrt{3}\times\sqrt{3})R30°$ phases, which is 1.4 in the experiment.

In order to derive the ground-state energy for the domain wall structure occurring at coverages higher than 0.25 ML as a function of coverage, we restricted the calculations to the one-dimensional domain-wall model in Fig. 3. However, the simulation of the complex diffraction pattern that was observed at this coverage required the random distribution of these domain walls on the surface as well as their simultaneous orientation along all three possible crystallographic orientations.[13] This model thus neglects wall crossing ener-

gies as well as contributions from end points of domain walls. However, we will show below that the coverage dependence of the energy derived for the one-dimensional domain-wall model describes the data from the simulations very well. In addition, and in agreement with experiment, a random two-dimensional network of domain walls was also observed in the simulations using the best-fit parameter values, as described below.

The easiest way to calculate the energy per adsorbate atom ϵ for the domain-wall structure is to sum up all energy contributions from the atoms within the pseudo unit mesh shown in Fig. 3(b). Let $1/w$ be the average number of rows with fcc site occupation between two domain walls. w can therefore be interpreted as the density of domain walls. $w=0$ corresponds to the ordered $p(2\times2)$ structure with oxygen on fcc sites and $w=1$ to the maximum density of domain walls at a coverage of 1/3 MD [Fig. 3(c)] with equal occupation of fcc and hcp sites. The coverage as a function of w is given by

$$\Theta=\frac{w+1}{2(w+2)}. \tag{3}$$

For the energy per adsorbate atom ϵ_{DW} of the domain-wall structure one gets

$$\epsilon_{\mathrm{DW}}(w)=\frac{w}{1+w}\left[h+3e_4+\left(\frac{3}{w}-1\right)e_6\right]. \tag{4}$$

Using Eq. (3), Eq. (4) can be rewritten as

$$\epsilon_{\mathrm{DW}}(\Theta)=(h+3e_4)\left(2-\frac{1}{2\Theta}\right)+\left(\frac{2}{\Theta}-5\right)e_6. \tag{5}$$

At a coverage of 1/3, a $(\sqrt{3}\times\sqrt{3})R30°$ phase is observed in the experimental phase diagram at low temperatures. Therefore, the $(\sqrt{3}\times\sqrt{3})R30°$ structure must have a lower ground-state energy than the domain-wall phase at this coverage. This leads to

$$h+3e_4+2e_6>6e_5. \tag{6}$$

On the other hand, the domain-wall structure should occur at coverages between 0.25 and 0.30 ML instead of the alternative, a coexistence of $p(2\times2)$ and $(\sqrt{3}\times\sqrt{3})R30°$ structures.[4,17] In order to calculate the condition for the occurrence of the domain-wall phase in the energetic ground state the ground-state energies of the domain-wall phase and the coexistence of the $p(2\times2)$ and the $(\sqrt{3}\times\sqrt{3})R30°$ phase must be compared. The latter is given by

$$\epsilon_{\mathrm{mix}}(\Theta)=6e_5\left(2-\frac{1}{2\Theta}\right)+e_6\left(\frac{3}{\Theta}-9\right). \tag{7}$$

In order to stabilize the domain-wall structure at a coverage above 0.25 ML

$$\frac{d\epsilon_{\mathrm{DW}}}{d\Theta}<\frac{d\epsilon_{\mathrm{mix}}}{d\Theta} \tag{8}$$

has to be fulfilled since

$$\epsilon_{\mathrm{DW}}\left(\Theta=\frac{1}{4}\right)=\epsilon_{\mathrm{mix}}\left(\Theta=\frac{1}{4}\right). \tag{9}$$

Inserting Eqs. (5) and (7) into Eq. (8) leads to

$$h+3e_4+2e_6<6e_5. \tag{10}$$

Obviously, Eqs. (6) and (10) cannot both be fulfilled at zero temperature, i.e., it is not possible to stabilize the ground states of the one-dimensional domain-wall phase shown in Fig. 3 at coverages $\Theta>0.25$ and a $(\sqrt{3}\times\sqrt{3})R30°$ phase at a coverage of 1/3 simultaneously. This does not mean, however, that the model fails or that more interactions have to be taken into account, since both experiment and simulation are carried out at finite temperatures. The entropy gain of the domain-wall phase compared to the coexistence of $p(2\times2)$ and $(\sqrt{3}\times\sqrt{3})R30°$ phases can therefore lead to the same sequence of phases as found in the experiment at low temperatures. This seems to be the reason why our simulations using the model given above actually reproduces the experimentally observed sequence of phases, a $p(2\times2)$ phase, the domain-wall phase, a coexistence of the domain-wall phase with a $(\sqrt{3}\times\sqrt{3})R30°$ phase, and the pure $(\sqrt{3}\times\sqrt{3})R30°$ phase, even at the lowest accessible temperatures.

Relations (2) and (6) define exact conditions for the possible range of interactions. It turned out that the experimental phase diagram can be reproduced with $e_6=0$ at coverages between 0.25 and 0.333 ML. In order to keep the number of free parameters as small as possible, we set e_6 to zero. To reproduce the experimentally observed $p(2\times2)$ islands at low coverages a weak attractive interaction e_6 is necessary. Estimates from simulations using a similar model show that $e_6\leqslant0.04e_2$ would suffice to reproduce the experimental phase diagram completely. This small contribution of e_6 would also slightly reduce e_5 [see Eqs. (2) and (6)], but would not change the topology of the phase diagram at coverages $\Theta>0.25$. Since we are primarily interested in the coverage range between 0.25 and 0.333 ML, we did not consider this small attractive interaction. Explicit test calculations at $T=0.04e_2/k$ and $e_6=0$ showed that the experimentally observed sequence of phases is still observed if $h+3e_4$ exceeds $6e_5$ by less than 20%.

The remaining three parameters can be fitted using additional experimental information. It turned out in the simulations that the binding-energy difference between fcc and hcp sites can be determined by comparing the occupation probabilities of fcc and hcp sites at the ideal coverage of the $p(2\times2)$ phase with the experimental values. These were determined very recently by analyzing LEED $I(E)$ curves.[12] In Fig. 4 the variation of these occupation probabilities as a function of the reduced temperature $(T-T_c)/T_c$ is shown for different values of the binding-energy difference h. In these simulations, e_5 was set to $0.12e_2$, a value that not only fulfills Eq. (2), but also allows an optimal fit of the phase diagram. e_4 was set to a value slightly larger than $2e_5-h/3$ (see above). Both in experiment and in the simulations an S-shaped curve with a maximum slope at the critical temperature of the order-disorder phase transition was found for the occupation probabilities. With the other parameters preset as described, the best agreement with experiment was achieved for a value of $h=0.17e_2$. Note that well below the critical temperature only fcc sites are occupied independent of the value of the binding-energy difference between fcc and hcp sites. Therefore, a structural analysis of the ordered

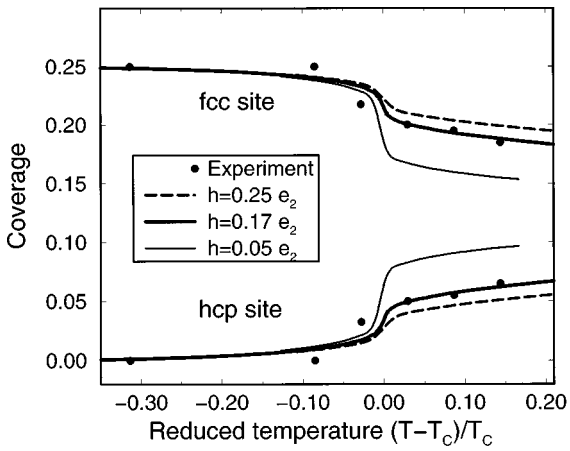

FIG. 4. Coverage of adsorbate atoms in fcc and hcp sites as a function of the reduced temperature $(T-T_c)/T_c$. Lines are data from simulations assuming a different binding-energy difference of fcc and hcp sites. Filled circles are experimental data. For details, see the text.

layer does not contain any information about the binding-energy difference of different adsorption sites. Finally, e_5 and e_4 were optimized by fitting the relative critical temperatures of the $p(2\times2)$ and the $(\sqrt{3}\times\sqrt{3})R30°$ structure and simultaneously reproducing the correct coverage dependence of observed phases at low temperatures. For given values of h and e_5, e_4 is almost completely determined by the condition that the domain-wall structure must occur at coverages larger than 0.25 and the $(\sqrt{3}\times\sqrt{3})R30°$ structure at a coverage of 1/3. For instance, for $e_5=0.12e_2$ and $h=0.17e_2$, we found the coexistence of $p(2\times2)$ and $(\sqrt{3}\times\sqrt{3})R30°$ phases for $e_4>0.25e_2$ and no $(\sqrt{3}\times\sqrt{3})R30°$ structure for $e_4<2e_5-h/3=0.183e_2$, as obvious from Eq. (6). This limits the allowed range of e_4 to the interval $e_4=0.21e_2\pm15\%$.

Finally, we will briefly discuss the allowed range for the interaction e_3 in order to maintain the topology of the phase diagram. A lower bound for e_3 can be derived from the condition that a $(\sqrt{3}\times\sqrt{3})R30°$ structure exists at a coverage of 1/3. As an alternative configuration, we could cover the surface with a $p(2\times2)$ structure in fcc sites and add excess atoms randomly on hcp sites in the center of the $p(2\times2)$ unit cells. In this structure, every hcp atom produces three pairs of adatoms with a distance corresponding to the interaction e_3. For the case $e_6=0$, the energy per adsorbate atom of this structure is given by

$$\epsilon=\frac{3}{4}e_3+\frac{h}{4}. \tag{11}$$

Since the energy of the $(\sqrt{3}\times\sqrt{3})R30°$ structure must be lower at this coverage, we get a lower bound for the interaction e_3:

$$e_3>4e_5-h/3. \tag{12}$$

Using the best-fit values ($e_5=0.12$ and $h=0.17$), we see that the assumed value of $0.66e_2$ is well above the lowest possible value of $0.43e_2$ given by Eq. (12).

The best fit to the phase diagram was finally achieved with the values given in Table I. Absolute energies given in eV are calculated by comparing the critical temperature of the order-disorder phase transition of the $p(2\times2)$ structure, $kT_c=0.141e_2$, with the experimental value $T_c=440$ K. The final simulated phase diagram is shown in Fig. 5. In addition to the structures found in the simulation, a coexistence of the $p(2\times2)$ and the $(\sqrt{3}\times\sqrt{3})R30°$ structure postulated by the ground-state calculations described above is shown schematically at very low temperatures.

TABLE I. Final result for the interaction energies used for the simulation of the phase diagram in Fig. 5.

Interaction	Energy e_i/e_2	Energy (eV)
e_1	∞	
e_2	1.000	0.270
e_3	0.667	0.180
e_4	0.210	0.057
e_5	0.120	0.032
e_6	0.000	0.000
h	0.170	0.046

IV. TEST OF GEOMETRIC CONFIGURATIONS

For the simulation to be trustworthy, not only must the phase diagram be reproduced, but also all experimentally known structural details should agree with experiment. The most sensitive range with respect to structural changes is again the coverage range between 0.25 and 0.33. In the following, we will show that also the structural details obtained from the simulation, with the parameters optimized as described above, are in good agreement with our experimental results. This comprises, in particular, the structure with only short-range-ordered domain walls. As we will show, this structure is in fact only stabilized by entropy. In Fig. 6 the simulated diffraction pattern at a coverage of 0.31 ML is compared with the experimental pattern measured at an elec-

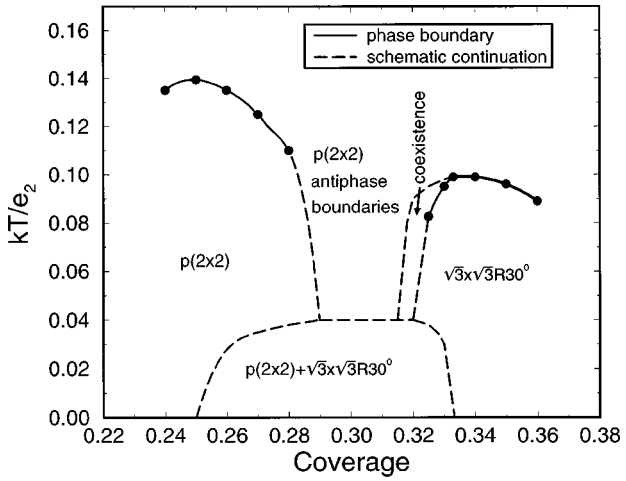

FIG. 5. Simulated phase diagram using the parameter set in Table I. Filled circles are data from the simulation. The solid lines connect the data points and serve as a guide to the eye. On the dashed lines, the sequence of ordered phases was checked, but the exact temperature dependence was not determined. Coexistence of the $p(2\times2)$ and the $(\sqrt{3}\times\sqrt{3})R30°$ phases was postulated from the ground-state calculations, but was not observed in the simulations for this parameter set at temperatures $kT>0.05e_2$.

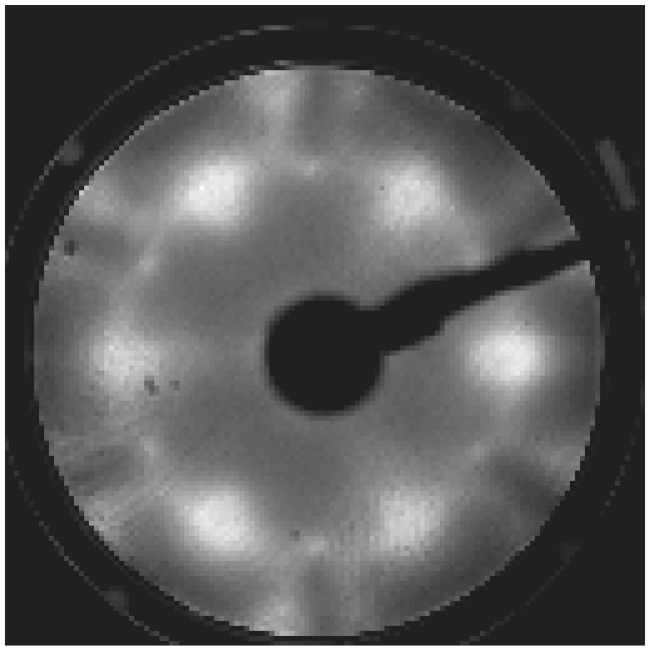

(a)

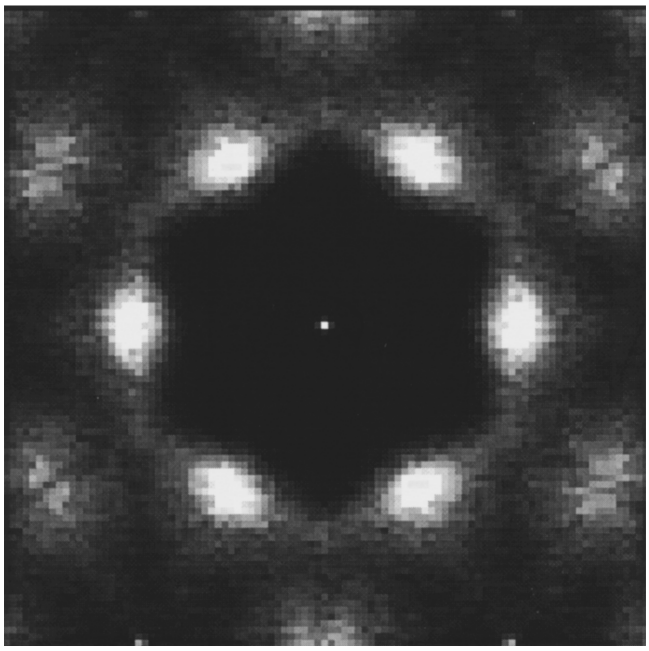

(b)

FIG. 6. Left image: experimental diffraction pattern of O/Ni(111) at a coverage of about 0.31 ML and an electron energy of 45 eV. Right image: simulated diffraction pattern at a coverage of 0.31 ML and a temperature $kT=0.08$.

tron energy of 45 eV. The characteristic features of the experimental diffraction pattern are well reproduced. The characteristic shape of the (1/2,0) spot and the streaky split (1/2,1/2) spot can be observed in both simulation and experiment. However, the splitting of the (1/2,1/2) spot is larger in the experimental diffraction pattern, most likely due to a small error in the experimental coverage determination. In agreement with the experimental phase diagram, also a coexistence of the $(\sqrt{3}\times\sqrt{3})R30°$ phase and the domain-wall structure was found in the experiment at a coverage of about

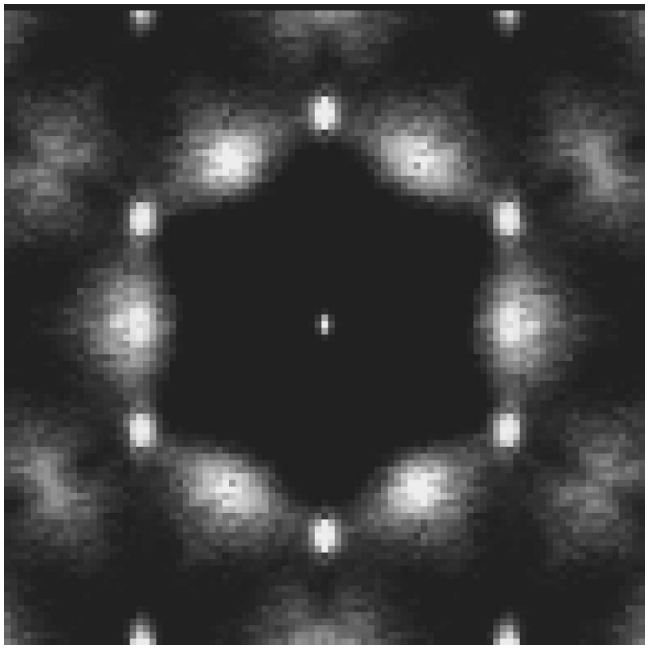

FIG. 7. Simulated diffraction pattern at a coverage of 0.32 ML and a temperature $kT=0.07$. A coexistence of the $(\sqrt{3}\times\sqrt{3})R30°$ phase and the domain-wall structure can be observed.

0.32 ML. The corresponding simulated diffraction pattern is shown in Fig. 7. In addition to the characteristic diffraction pattern of the domain-wall structure, diffraction spots of the $(\sqrt{3}\times\sqrt{3})R30°$ structure can be clearly seen.

In our LEED study,[13] we have shown that the diffraction pattern of Fig. 6 can be produced by a surface containing $p(2\times2)$ domains with oxygen adsorbed in fcc sites that are separated by a random distribution of domain walls in which hcp sites are occupied. In the LEED analysis, the type of domain walls were identified as those shown in Fig. 3. It is interesting to see whether these domain walls also occur in the Monte Carlo simulations. A typical snapshot of the surface at a coverage of 0.28 ML using a very small system size (24×12 sites) is shown in Fig. 8. A large part of the surface is covered by $p(2\times2)$ domains with oxygen atoms in fcc sites. These $p(2\times2)$ domains are separated by domain walls in which the hcp site is occupied. The width of the domain walls is always only a single atomic row. It can be further seen that different domain walls are aligned along different directions simultaneously. This observation is also in agreement with the experiment since the experimental diffraction pattern can only be explained by a random distribution of domain walls aligned along all possible crystallographic directions on the surface. The observation of the local surface structure also corroborates the restriction to the one-dimensional (1D) model used to calculate the ground-state energies of competing phases. In order to judge the quantitative agreement between the analytic calculations for the 1D domain-wall model and the simulations, the ground-state properties of the domain-wall model are compared to the simulations at relatively low temperatures ($T=0.07e_2/k=220$ K). Figure 9 shows the relative coverage in fcc and hcp sites as a function of the total coverage. The lines are the analytic expressions for the domain-wall model given by

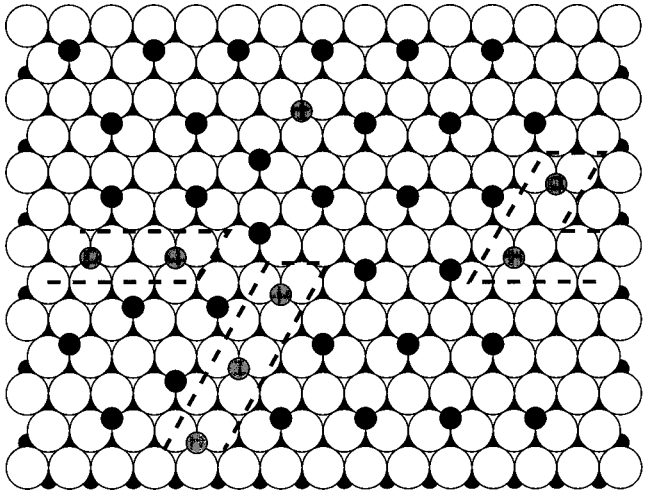

FIG. 8. Typical snapshot of the simulated surface at a coverage of 0.28 ML using a system size of 24×12 sites. $p(2\times2)$ domains with oxygen in fcc sites (black-filled circles) are separated by a random distribution of domain walls in which hcp sites (gray-filled circles) are occupied. The domain walls are shown as dashed lines.

$$\frac{\Theta_{\mathrm{fcc}}}{\Theta}=\frac{1}{2\Theta}-1 \quad \frac{\Theta_{\mathrm{hcp}}}{\Theta}=1-\frac{\Theta_{\mathrm{fcc}}}{\Theta}. \tag{13}$$

The agreement is obviously very good for the coverages below 0.3. Deviations from the analytic prediction are due to the formation of local regions with $(\sqrt{3}\times\sqrt{3})R30°$ periodicity. In these regions only fcc sites are occupied, which obviously reduces the relative coverage in hcp sites.

Since the domain walls are not perfectly straight and also have end points with a different local structure than within the domain walls, the contributions of these terms to the total energy is difficult to estimate. Therefore, also the simulated energy per adsorbate atom as a function of coverage was compared with the ground-state energy of the 1D domain-wall model given by Eq. (5). The data from the simulation together with the analytic prediction are shown in Fig. 10. Up to a coverage of about 0.31 ML the simulated energies are slightly larger, showing a small energy increase due to

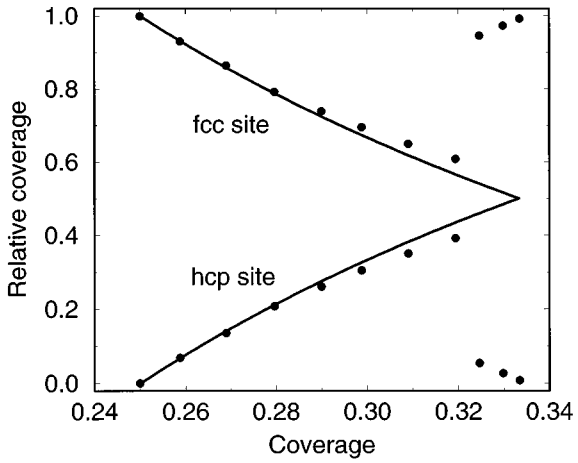

FIG. 9. Relative coverage $\Theta_{\mathrm{fcc}}/\Theta$ ($\Theta_{\mathrm{hcp}}/\Theta$) in fcc (hcp) sites as a function of coverage Θ. Filled circles are data from the simulations at a temperature $kT=0.07e_2$, the solid line is the prediction from the one-dimensional domain-wall model in Fig. 3.

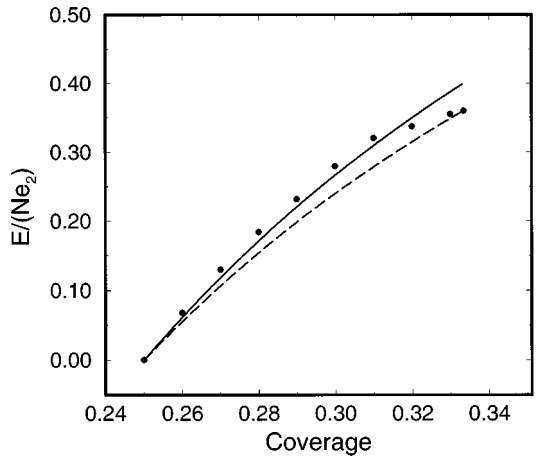

FIG. 10. Energy per adsorbate atom E/N as a function of coverage. Filled circles are data from the simulations at a temperature $kT=0.07e_2$, the solid line is calculated for the one-dimensional domain wall model [Eq. (5)]. The dashed line shows the coverage dependence of the energy per adsorbate atom E/N for the coexistence of $p(2\times2)$ and $(\sqrt{3}\times\sqrt{3})R30°$ phases calculated from Eq. (7).

meandering of domain walls and end-point contributions. At higher coverages the formation of $(\sqrt{3}\times\sqrt{3})R30°$ regions in coexistence with the domain-wall structure apparently lowers the energy. The analytic expression for the coexistence of $p(2\times2)$ and $(\sqrt{3}\times\sqrt{3})R30°$ structures is also shown in the figure. According to the analytic calculations described above, the ground-state energy for the coexistence of these two phases is always smaller than that of the domain-wall structure. Hence these data show clearly that the formation of the domain walls in thermal equilibrium is due to the entropic gain of the domain-wall structure compared to the coexistence of the two well-ordered structures even at temperatures as low as 220 K. Summarizing this section, the short-range-ordered domain-wall phase exists only as a thermally activated phase in this system, the ground state being either the coexistence of $p(2\times2)$ and $(\sqrt{3}\times\sqrt{3})R30°$ phases or the pure $(\sqrt{3}\times\sqrt{3})R30°$ phase. Nevertheless, also its structure on average is well described by the model presented above, which contains only repulsive pairwise interactions, as tested by calculating the structure factor of this phase and comparing it with experiment under various conditions.

V. DISCUSSION

Although still not free of ambiguities even within the lattice-gas model, our detailed optimization of the lateral interactions between oxygen atoms on the Ni(111) surface yields several remarkable results. First, it is obviously possible to get a fully satisfying fit to the experimental phase diagram in this system up to the maximum density of 0.33 by use of coverage-independent pairwise interactions without inclusion of n-particle ($n\geqslant3$) interactions. Invoking the equivalence of coverage-dependent geometrical relaxations and three- or more-particle interactions,[18] these relaxations must be small, in agreement with the findings in structural investigations of the pure $p(2\times2)$,[7] $(\sqrt{3}\times\sqrt{3})R30°$,[8] and short-range-ordered domain-wall phase.[13] These findings

also agree with other systems of atomic adsorbates in the low-coverage range, for which the phase diagram, the lateral interactions, and the geometric structure have been investigated in more detail, e.g., O (Refs. 16, 19, and 20) and S/Ru(0001).[4,21] Up to coverages between 0.33 [S/Ru(0001)] and 0.5, they also can be described by only pairwise interactions, which are independent of coverage. Correspondingly, the changes of the local geometry as a function of coverage were found to be smaller than 0.1 Å in these cases. The model Hamiltonian (1) already used in the Monte Carlo simulations to the same system by Roelofs *et al.*[6] thus gets its justifications by the geometrical information not available at that time.

Second, the detailed structural information now available also allowed us to check the quality of the fit by investigating in detail the agreement between experimental data and simulation for the domain wall phase, a question not addressed in the earlier study. Thus, although the interaction energies used in Ref. 6 are in the same range as ours, it turns out that by considering Eqs. (6)–(10) the parameter set used in Ref. 6 cannot correctly reproduce the short-range-ordered domain-wall phase. In addition, the information about site occupation probabilities allows a determination of the difference binding energies h. This difference was determined close to the order-disorder transition of the low-coverage $p(2\times2)$ phase. It is clear from the above description that h depends also mainly on e_4 and e_5, which are, however, restricted by Eqs. (6) and (10), by the best fit of the phase diagram and by the correct sequence of ordered phases. The remaining variability limits the accuracy of our best fit to about 20% within the given model, not taking into account the uncertainty due to e_3, which was not varied systematically. The use of additional experimental information, therefore, was crucial to remove some of the ambiguities and to obtain more accurate estimates for the lateral interactions and the binding difference of fcc and hcp sites.

The value of around 50 meV obtained from the fit to the data (see Fig. 4) is about one order of magnitude smaller than the binding-energy difference between fcc and hcp sites calculated from first principles for O/Ru(0001) (Refs. 22 and 23) at a coverage of 0.25 ML. [On the Ru(0001) surface, the hcp site is energetically more favorable according to the common trend that oxygen preferentially adsorbs on the site an additional metal layer would occupy.[24]] This large difference seems to be reasonable since oxygen even occupies nearest-neighbor sites on Ru(0001) without fcc site occupation.[19] The formation of the domain-wall structure and the possibility of a thermally activated occupation of the energetically less favorable site is therefore a clear indication of a very small binding-energy difference between the two competing threefold hollow sites. A more quantitative comparison with calculations from first principles would certainly be very informative. This comparison could be extended to the lateral interactions. It is worth noting that their decrease as a function of distance in our case follows closely an exponential. A reversal of sign occurs at a distance of 2 lattice constants (e_6), but our accuracy is not sufficient to see any indication for oscillatory behavior at larger distances or to determine the behavior at large distances, for which predictions exist.[25]

Third, the comparison of ground-state energies of the domain-wall phase (both in the model and in the simulation) with the competing ordered phases revealed not only that the experimentally observed sequence of phases as a function of coverage are observed in a very small area in the parameter space, but that the ground-state should always phase separate. No experiment has been done at sufficiently low temperatures to confirm this prediction. It might also be hard to verify due to low mobilities of the adsorbate and consequent incomplete demixing.

The critical properties of the order-disorder phase transition of the $p(2\times2)$ phase is still somewhat controversial since the three investigations published[9–11] yielded three different results, while there is no doubt about the $(\sqrt{3}\times\sqrt{3})R30°$ transition to be first order in this system. Two of them[9,11] claim the transition to be continuous, although with different critical exponents (exponents close to the Ising class[9] and four-state Potts exponents,[11] respectively). In the third study[10] a transition was found that was weakly first order. While these different results can be caused by the influence of impurities and other defects,[26–28] a conclusive reason for these discrepancies has not been given at present. Even the results with the ''expected'' four-state Potts exponents might be questionable because of the abnormally low Debye temperature used in this evaluation of critical exponents, which is at variance with optimizations of the Debye temperature in LEED analyses of the thermally disordered system.[13]

We have carried out simulations of the critical properties of this phase transition with the parameter set optimized as described above (i.e., with $e_6=0$).[29] Up to 10^6 MC sweeps were used and the system size varied between 24×48 and 60×120 lattice sites. The results show that the transition is indeed no longer continuous, but very weakly first order. From the finite-size scaling analysis we obtained values for $\alpha/\nu=1.16$ and $\gamma/\nu=1.90$, which are still not far from the values of the continuous four-state Potts transition ($\alpha/\nu=1$ and $\gamma/\nu=1.75$). The value for γ/ν obtained from the simulation, however, would also be compatible with 2, the value for a first-order transition. The exponent ν determined from the shift of T_c as a function of system size both for data of the susceptibility and of the specific heat was 0.53 ± 0.05, which also points towards first order. Plots of the specific heat and the susceptibility for the largest system size investigated show crossover behavior for the data above T_c with effective exponents corresponding to first-order exponents close to T_c, whereas the data below T_c (outside the finite-size regime) can be fitted best with exponents $\alpha=1$ and $\gamma=2$ over more than one order of magnitude in reduced temperature. An indication for a weak first-order phase transition is also the ratio of amplitudes χ_+/χ_- of the susceptibility above and below T_c, respectively. Depending on temperature, values between 3 and 8 were obtained, far away from the value of 40 derived from simulations of the four-state Potts model.[30] No pure power-law behavior was observed for the order parameter. On the other hand, plots of the energy per adatom still yield the value of the four-state Potts class ($\alpha=0.672$).

From these results we conclude that, similar to our experimental results, we found a weak first-order phase transition of the $p(2\times2)$ phase to disorder also in the simulations. There is still the open question, which was not investigated

in this context, whether this result holds for the whole phase boundary of the $p(2\times2)$ phase. We cannot rule out, however, the possibility of a critical end point at a coverage of 0.25. The tendency towards first order will certainly be enhanced by an attractive interaction e_6 so that the results of Roelofs *et al.*,[6] who found with their parameter sets only first-order transitions, would be fully compatible with our findings. The fact that the system both in simulations and in the experiment is only marginally of first order makes it particularly interesting, but also susceptible to small distortions by imperfections, especially on the experimental side.

VI. CONCLUSION

Summarizing, we have, for a rather complicated adsorption system O/Ni(111), explored the possibility to make the determination of lateral interactions by simulation of the phase diagram more reliable by using extensively structural data as additional experimental input. This allows, first of all, us to justify the use of a lattice-gas model and to determine the symmetry and the number of adsorption sites. At the same time, the structural information from both experiment and simulation can be compared, which reduces the number of free parameters in the model drastically. The comparison of critical properties turns out not to be easy in this system since the phase transition of the $p(2\times2)$ phase is only weakly first order. Since the results of experiment and theory agree also in this respect, the lattice-gas model turns out to be indeed fully satisfactory and consistent.

ACKNOWLEDGMENTS

We would like to thank H.-U. Everts and I. Lyuksyutov for many helpful discussions. This work has been supported by the Deutsche Forschungsgemeinschaft through Project No. Pf238/5.

[1] F. Watanabe and G. Ehrlich, Phys. Rev. Lett. **62**, 1146 (1989).
[2] Ph. Ebert, Xun Chen, M. Heinrich, M. Simon, K. Urban, and M. G. Lagally, Phys. Rev. Lett. **76**, 2089 (1996).
[3] K. Binder and D. P. Landau, in *Molecule-Surface Interaction*, edited by K. Lawley (Wiley, New York, 1989).
[4] M. Sandhoff, H. Pfnür, and H.-U. Everts, Europhys. Lett. **25**, 105 (1994).
[5] A. R. Kortan and R. L. Park, Phys. Rev. B **23**, 6340 (1981).
[6] L. D. Roelofs, A. R. Kortan, T. L. Einstein, and R. L. Park, J. Vac. Sci. Technol. **18**, 492 (1981).
[7] E. Schmidtke, C. Schwennicke, and H. Pfnür, Surf. Sci. **312**, 301 (1994).
[8] M. A. Mendez, W. Oed, A. Fricke, L. Hammer, K. Heinz, and K. Müller, Surf. Sci. **253**, 99 (1991).
[9] L. D. Roelofs, A. R. Kortan, T. L. Einstein, and R. L. Park, Phys. Rev. Lett. **46**, 1465 (1981).
[10] L. Schwenger, C. Voges, M. Sokolowski, and H. Pfnür, Surf. Sci. **307-309**, 781 (1994).
[11] Z. Li, X. Liang, and R. D. Diehl, Surf. Sci. **327**, 121 (1995).
[12] C. Schwennicke, C. Voges, and H. Pfnür, Surf. Sci. **349**, 185 (1996).
[13] C. Schwennicke and H. Pfnür, Surf. Sci. **369**, 248 (1996).
[14] K. Kawasaki, in *Phase Transitions and Critical Phenomena*, edited by C. Domb and M. S. Green (Academic, New York, 1972), Vol. 5a.
[15] C. Voges, diploma thesis, University of Hannover, 1992 (unpublished).
[16] P. Piercy, K. de'Bell, and H. Pfnür, Phys. Rev. B **45**, 1869 (1992).
[17] R. Dennert, M. Sokolowski, and H. Pfnür, Surf. Sci. **271**, 1 (1992).
[18] B. N. J. Persson, Surf. Sci. Rep. **15**, 1 (1992).
[19] H. Pfnür, G. Held, M. Lindroos, and D. Menzel, Surf. Sci. **220**, 43 (1989).
[20] M. Lindroos, H. Pfnür, G. Held, and D. Menzel, Surf. Sci. **222**, 451 (1989).
[21] D. Jürgens, G. Held, and H. Pfnür, Surf. Sci. **303**, 77 (1994).
[22] C. Stampfl, S. Schwegmann, H. Over, M. Scheffler, and G. Ertl, Phys. Rev. Lett. **77**, 3371 (1996).
[23] C. Stampfl and M. Scheffler, Phys. Rev. B **54**, 2868 (1996).
[24] U. Starke, M. A. Van Hove, and G. A. Somorjai, Prog. Surf. Sci. **46**, 305 (1994).
[25] T. L. Einstein, in *Physical Structure of Solid Surfaces*, edited by W. N. Unertl, Handbook of Surface Science Vol. 2 (Elsevier, New York, 1996).
[26] S. Chen, A. M. Ferrenberg, and D. P. Landau, Phys. Rev. Lett. **69**, 1213 (1992).
[27] M. A. Novotny and D. P. Landau, Phys. Rev. B **32**, 3112 (1985).
[28] L. Schwenger, K. Budde, C. Voges, and H. Pfnür, Phys. Rev. Lett. **73**, 296 (1994).
[29] C. Schwennicke and H. Pfnür (unpublished).
[30] N. C. Bartelt, T. L. Einstein, and L. D. Roelofs, Phys. Rev. B **35**, 1776 (1987).